Biochimica et Biophysica Acta 1808 (2011) 1985–1992

Contents lists available at ScienceDirect

Biochimica et Biophysica Acta

journal homepage: www.elsevier.com/locate/bbamem

Ionization properties of mixed lipid membranes: A Gouy–Chapman model of the electrostatic–hydrogen bond switch

Demmelash H. Mengistu [a], Edgar E. Kooijman [b], Sylvio May [a,*]

[a] Department of Physics, North Dakota State University, Fargo, ND 58108–6050, USA
[b] Department of Biological Sciences, Kent State University, Kent, OH 44242, USA

ARTICLE INFO

Article history:
Received 1 December 2010
Received in revised form 17 February 2011
Accepted 7 March 2011
Available online 13 March 2011

Keywords:
Lipid
Membrane
Hydrogen bond
Electrostatics
Gouy-Chapman
Poisson-Boltzmann
Phosphatidic acid

ABSTRACT

The dissociation state of phosphatidic acid (PA) in a lipid bilayer is governed by the competition of proton binding and formation of a hydrogen bond through a mechanism termed the electrostatic–hydrogen bond switch. This mechanism has been suggested to provide the basis for the specific recognition of PA by proteins. Even in bare lipid bilayers the electrostatic–hydrogen bond switch is present if the membrane contains lipids like phosphatidylethanolamine that act as hydrogen bond donors. In this case, the dissociation state (pK_a) of PA depends strongly on membrane composition. In the present work we incorporate the electrostatic–hydrogen bond switch mechanism into the Gouy–Chapman model for a membrane that is composed of PA and a hydrogen bond-donating zwitterionic lipid. To this end, our model integrates into the Gouy–Chapman approach a recently suggested electrostatic model for zwitterionic lipids. Hydrogen bond formation is incorporated phenomenologically as an additional non-electrostatic interaction between the phosphomonoester headgroup of PA and the zwitterionic lipid headgroup. We express the energetics of the composite membrane in terms of a free energy functional whose minimization leads to a modified non-linear Poisson–Boltzmann equation that we have solved numerically. Our calculations focus on the influence of the membrane environment on the dissociation state of PA. This influence can be expressed as a shift of the second pK_a of PA, which we calculate as function of membrane composition, following experimental observation. The shift is large and negative if PA is the minor component in the membrane, and it changes over four pH units as function of the mole fraction of PA in the membrane. In contrast, the shift of the second pK_a of PA remains small and is always positive if the zwitterionic lipid is unable to act as hydrogen bond donor. Hence, we find that the electrostatic–hydrogen bond switch mechanism regulates the dissociation state of PA with much greater sensitivity than would be possible based on a pure electrostatic regulation through the membrane potential.

1. Introduction

Lipid–protein interactions at the lipid headgroup–aqueous interface are often governed by electrostatic interactions where cationic protein domains bind to anionic lipids. In many cases this electrostatic interaction is further facilitated by specific structural features of the protein domain such that it fits neatly "around" the lipid headgroup. Important examples are the PH, PX, FYVE, and similar domains that bind to one of the seven naturally occurring polyphosphoinositides [1,2]. In other cases the electrostatic interaction is driven solely by the total electrostatic potential of the membrane, which can be modulated by the concentration of phosphatidylserine (PS) in the lipid bilayer [3]. In the case of the polyphosphoinositides the highly specific protein–lipid interactions are governed by the functionalized (phosphorylated) inositol headgroup, while for PS the interaction is found to be electrostatic due to its high abundance. Phosphatidic acid (PA), however, interacts with proteins via another mechanism.

Phosphatidic acid, like phosphatidylinositol-(4,5)-bisphosphate (PIP_2), is a minor component of biomembranes and thus has to be located in a sea of (mostly) PS and phosphatidylcholine (PC) by its binding proteins. This recognition is facilitated by the phosphomonoester headgroup that sits close to the headgroup–acyl chain interface. Recently it was suggested that the phosphomonoester acts as an electrostatic–hydrogen bond switch allowing for highly specific electrostatic and hydrogen bond interactions [4]. The phosphomonoester headgroup of PA has two ionization constants, with the pK_{a2} located in the physiological pH range. Qualitatively the electrostatic–hydrogen bond switch model is best described as follows: When the "first" proton dissociates from the phosphomonoester headgroup, the "second" becomes more tightly bound due to the resulting negative charge and already present covalent interaction (see Fig. 1). Importantly, hydrogen bonds formed with the phosphomonoester compete for electrons and thereby destabilize the "second" proton, facilitating its dissociation (see Fig. 1). Kooijman and coworkers thus

* Corresponding author. Tel.: +1 701 231 7048.
E-mail address: sylvio.may@ndsu.edu (S. May).
URL: http://www.ndsu.edu/physics/people/faculty/may/ (S. May).

0005-2736/$ – see front matter © 2011 Elsevier B.V. All rights reserved.
doi:10.1016/j.bbamem.2011.03.001

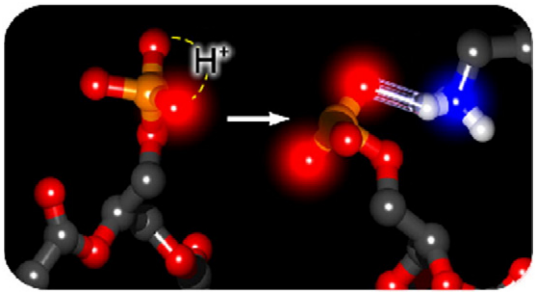

Fig. 1. Cartoon of the electrostatic–hydrogen bond switch. PA carrying one negative charge is shown on the left (charged oxygen is (high)lighted red). Shown is the "second" proton now bound by both electrostatic and non-electrostatic interactions. Interaction with a primary amine is shown on the right (charged nitrogen is (high) lighted blue), facilitating deprotonation of the phosphomonoester headgroup of PA via hydrogen bond formation. Carbons are colored gray, nitrogen is blue, oxygen is red, phosphorus is orange, and explicit protons are white. Taken with permission from Kooijman and Testerink [5].

proposed that PA-binding proteins exploit this property of the phosphomonoester of PA [4]. These proteins are attracted to the anionic membrane through electrostatic interactions where their PA binding domain binds transiently to anionic phospholipids. However, only when the PA binding domain locates the phosphomonoester of PA it is able to dock onto the membrane, namely by displacing the "second" proton (assuming it possessed a single negative charge before binding) in the phosphomonoester of PA. This creates a specific and strong electrostatic interaction (now based on two negative charges) that is further strengthened by hydrogen bond interactions since the fully dissociated phosphomonoester acts as an efficient hydrogen bond acceptor.

The electrostatic–hydrogen bond switch mechanism predicts that the pK_{a2} of PA depends sensitively on the ratio between PC and phosphatidylethanolamine (PE), and hence the location of PA in the cell. Furthermore, the model predicts that PA–protein interaction will be sensitive to intracellular pH, exactly as was recently shown by Loewen and coworkers [6]. Namely, they showed that Opi1, a transcriptional regulator, binds to the ER at neutral pH and comes off the ER as the pH decreases based on the metabolic state of the cell. The work by Loewen et al. effectively links metabolism to membrane biogenesis with PA acting as a pH sensor according to the electrostatic–hydrogen bond switch mechanism. The goal of the current work is to use the classical Gouy–Chapman model to develop a theoretical description of the electrostatic–hydrogen bond switch, specifically as it depends on local lipid composition and pH.

Classical Gouy–Chapman theory is frequently used to account for the diffuse double layer near charged surfaces (including lipid membranes) on a mean-field level [7,8]. The model leads to the Poisson–Boltzmann equation (a non-linear differential equation) that can be solved numerically or, in some cases, even analytically [9,10]. In the most simple case, the surface charge density σ of a given surface immersed in a salt-containing aqueous solution is fixed, but it is also possible to include additional degrees of freedom, such as ionization equilibria [11], mobile charges within a laterally inhomogeneous surface [12], polyelectrolytes [13], hydration models of water [14], and the presence of mobile dipoles in the aqueous solution [15]. Recently, a model was suggested to account for the electrostatic properties and orientational freedom of zwitterionic headgroups in a mixed lipid membrane [16]. In this model, the zwitterionic headgroup is represented simply by two opposite charges, a negative charge located at the polar/apolar interface and a positive charge, at fixed distance away from the first, being able to move on a hemispherical surface inside the polar (i.e. headgroup) region. This model, which is simple enough to allow for some analytical solutions [17,18], has been used recently to investigate thermodynamic properties of anionic and cationic membranes [16], electrostatic interactions of mixed membranes with macroions [19], binding of DNA to zwitterionic membranes mediated by divalent cations [20], and ionization properties of mixed anionic–zwitterionic membranes[21]. In all these studies, the zwitterionic lipid interacted with the environment only electrostatically, and the possible presence of non-electrostatic interactions was assumed to be completely independent (i.e., not coupled with the electrostatic interactions). Developing a Gouy–Chapman framework that consistently incorporates the coupling between electrostatic and non-electrostatic interactions for a mixed anionic–zwitterionic lipid bilayer is a major goal of the present work.

The electrostatic–hydrogen bond switch influences the ionization properties of a phosphomonoester headgroup through the competition of proton binding and formation of a hydrogen bond. The equilibrium of this process is influenced by the ambient electrostatic conditions (salt and pH). Different chemical moieties may act as hydrogen bond donors, including the hydroxyl group of lysophosphatidic acid [22], positively charged side chains (lysine, arginine) of membrane-interacting peptides [4], or the primary amine group of phosphatidylethanolamine [22]. The latter involves a zwitterionic lipid and thus lends itself to be integrated into the electrostatic Gouy–Chapman model for mixed anionic–zwitterionic membranes discussed above.

As model system we take a mixed anionic–zwitterionic lipid bilayer consisting of PA and PE, and contrast the results with those for PA and PC. We also emphasize that the Gouy–Chapman model is not based on an atomistic representation of the involved lipids, and its scope is not to quantitatively reproduce the ionization properties of a specific system. Instead, our approach represents a minimal model that only accounts for the essential structural and energetic features of the membrane. Minimal models such as the present one typically have only few parameters. These can be varied systematically which allows a complete understanding and transparent interpretation of the physical behavior described by the model. Besides modeling the electrostatic–hydrogen bond switch, the present study also demonstrates an example of incorporating non-electrostatic interactions into the Gouy–Chapman model.

2. Model

We consider a planar binary lipid bilayer that consists of a two-component mixture: a lipid carrying a phosphomonoester and a zwitterionic lipid that is able to interact with the phosphomonoester via the formation of a hydrogen bond. A specific realization of such a system is a mixture of PA and PE to which we will refer in the following. We will also consider the case that no hydrogen bond can form; the zwitterionic lipid would then represent, for example, PC which has a quaternary amine in its headgroup that does not act as hydrogen bond donor. We shall denote the mole fraction of PA by ϕ. The mole fraction of the zwitterionic lipid (either PE or PC) is thus $1-\phi$.

PA exhibits a variable dissociation state of its phosphomonoester headgroup. Of the two pK values, only the second falls within the physiological pH range. Hence PA is usually found carrying either one or two negative charges, which we denote by PA^- and PA^{2-}, respectively. In the following we focus only on these two ionization states, with PA having either one or two headgroup charges. We denote the fraction of PA^{2-} vs. PA^- by $\eta/(1-\eta)$ where η denotes the degree of deprotonation (with $0\leq\eta\leq1$). The lipid bilayer can then be viewed as a quasi-ternary system with mole fractions $\phi\eta$ of PA^{2-}, $\phi(1-\eta)$ of PA^-, and $(1-\phi)$ of the zwitterionic lipid (PE). The lipid mole fraction ϕ is usually an experimentally given quantity, but the degree of deprotonation η will adjust so as to minimize the total free energy of the bilayer. Fig. 2 illustrates the system.

Poisson–Boltzmann theory is a mean-field model where all charges are point like, irrespective of whether they are part of a proton, salt ion, or lipid. However, the headgroup of the zwitterionic

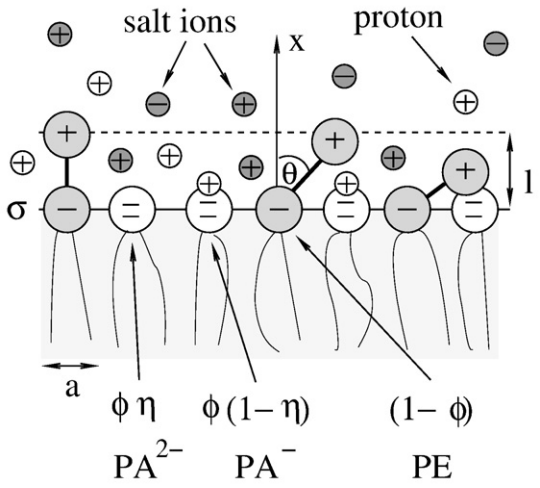

Fig. 2. Illustration of a mixed acidic–zwitterionic lipid layer, consisting of PA and PE. The mole fractions of PA^{2-}, PA^{-}, PE are $\phi\eta$, $\phi(1-\eta)$, $1-\phi$, respectively, where η denotes the degree of deprotonation of PA. The charges of PA^{2-} and PA^{-} as well as the negative charge of PE are confined to the plane $x=0$ whereas the positive charge of PE is able to reside at any position $x=l\cos\theta$ within the headgroup region ($0\le x\le l$), corresponding to a headgroup tilt angle θ. The cross-sectional area per lipid a is assumed to be constant, adopting the same value for all lipids. Charges belonging to the PE headgroups and salt ions are shaded. The horizontal broken line marks the outer boundary of the headgroup region at distance l away from the polar–apolar interface, $x=0$. The aqueous solution contains protons and monovalent salt ions.

lipid (PE) consists of two opposite charges that are well separated and cannot be condensed into one single point. To account for the structure of the zwitterionic headgroup we will adopt a model that has been introduced and analyzed in previous work [16]. Briefly, the headgroup is represented by two opposite charges that are separated by a fixed distance l. The negative charge resides strictly at the polar–apolar interface of the lipid layer, which we locate at position $x=0$ of a Cartesian coordinate system with the x-axis pointing normal to the lipid layer. The position of the positive charge is variable, allowing for headgroup tilt angles θ with $0\le\theta\le\pi/2$ (see Fig. 2). Instead of using the angle θ, it is more convenient to describe the headgroup tilt by the position $x=l\cos\theta$ of the positive headgroup charge along the x-axis. Obviously, $x=0$ for $\theta=\pi/2$ and $x=l$ for $\theta=0$. Generally, different x will be adopted with different probabilities. We denote the corresponding probability distribution by $P(x)$, normalized according to

$$\frac{1}{l}\int_0^l P(x)\mathrm{d}x = 1. \tag{1}$$

Note that for an unperturbed headgroup all orientations θ occur with the same probability, implying $P(x)=1$. We also note that P (and similarly all other physical quantities) depends only on the x-coordinate but—within the present mean-field approach—is invariant along the y, z-plane.

We assume the lipid membrane is immersed in an aqueous solution that contains monovalent salt ions and protons. The local concentrations of positively charged salt ions, negatively charged salt ions, and protons are denoted by $n_+=n_+(x)$, $n_-=n_-(x)$, and $n_\mathrm{p}=n_\mathrm{p}(x)$, respectively. The corresponding bulk values are n_0 (for the positive salt ions), $n_0+n_\mathrm{p}^0$ (for the negative salt ions), and n_p^0 (for the protons), thus ensuring electrical neutrality in the bulk. With these definitions we are able to specify the volume charge density $\rho(x)$ along the x-axis;

$$\frac{\rho(x)}{e} = \begin{cases} n_+ + n_\mathrm{p} - n_- + \dfrac{(1-\phi)}{al}\,P(x), & 0<x<l \\ n_+ + n_\mathrm{p} - n_-, & l\le x<\infty \end{cases} \tag{2}$$

where a denotes the cross-sectional area per lipid (assumed to adopt the same constant value for all lipids) and e is the elementary charge. The final term of Eq.(2) in the headgroup region $0<x<l$ describes the contribution from the positive charges of the zwitterionic headgroups. The negative charges from PA and from the phosphate groups of the zwitterionic lipids (PE) all reside at the polar/apolar interface of the lipid layer, $x=0$ (which we assume to be sharp). The corresponding surface charge density

$$\sigma = -\frac{e}{a}(1+\phi\eta), \tag{3}$$

located at $x=0$, has thus two contributions, $-(1-\phi)e/a$ from the zwitterionic lipids and $-\phi(1+\eta)e/a$ due to the presence of PA (where the yet unknown η reflects the dissociation equilibrium $PA^- \rightleftharpoons PA^{2-}+p^+$).

According to the electrostatic–hydrogen bond switch model, the phosphomonoester headgroup of PA is able to form a hydrogen bond with the zwitterionic headgroup of PE (or, more generally, with any other hydrogen bond donor) which increases the deprotonation state of PA. Using a phenomenological approach like the Gouy–Chapman model it is not obvious how to account for hydrogen bonds and the partial charge distributions in the involved lipids that cause the electrostatic–hydrogen bond switch mechanism. Nevertheless, we suggest to use an empirical non-electrostatic attractive potential (denoted by $-U(x)$ with $U(x)\ge 0$ and measured in units of the thermal energy $k_\mathrm{B}T$ where k_B is the Boltzmann constant and T the absolute temperature) that mimics the formation of a hydrogen bond. Specifically, if the distance, measured along the x-axis, of the hydrogen bond donor (i.e., the positive end of the zwitterionic headgroup of PE) is closer to the headgroup of PA^{2-} than a certain distance $\tilde{l}$ (with $\tilde{l}<l$), a hydrogen bond of strength $U_0>0$ (measured in units of $k_\mathrm{B}T$) forms. This amounts to the choice of the square-well potential

$$U(x) = \begin{cases} U_0, & 0<x<\tilde{l} \\ 0, & \tilde{l}\le x<\infty \end{cases} \tag{4}$$

which we adopt in the present work. We shall also model the situation that the zwitterionic headgroup cannot act as a hydrogen bond donor; PC is an example. In this case we set $U_0=0$. We note that in molecular simulations a 10–12 interaction potential is frequently used to model the formation of a hydrogen bond [23]. We discuss the 10–12 interaction potential and its relation to $U(x)$ (see Eq. (4)) in Appendix A.

The basis of our model is the following mean-field expression for the average free energy f per lipid, expressed in units of the thermal energy $k_\mathrm{B}T$,

$$\begin{aligned} \frac{f}{k_\mathrm{B}T} = {} & \frac{a}{8\pi l_\mathrm{B}}\int_0^\infty \mathrm{d}x\,(\Psi'(x))^2 \\ & + a\int_0^\infty \mathrm{d}x\left[n_+ ln\frac{n_+}{n_0} - n_+\right] \\ & + a\int_0^\infty \mathrm{d}x\left[n_- ln\frac{n_-}{n_0+n_\mathrm{p}^0} - n_-\right] \\ & + a\int_0^\infty \mathrm{d}x\left[n_\mathrm{p} ln\frac{n_\mathrm{p}}{n_\mathrm{p}^0} - n_\mathrm{p}\right] \\ & + \phi\left[\eta\, ln\frac{\eta}{\eta_0} + (1-\eta) ln\frac{1-\eta}{1-\eta_0}\right] \\ & + (1-\phi)\frac{1}{l}\int_0^l \mathrm{d}x\,P(x) lnP(x) \\ & - \eta\,\phi(1-\phi)\frac{1}{l}\int_0^l \mathrm{d}x\,P(x)U(x). \end{aligned} \tag{5}$$

The first term in Eq. (5) describes the total electrostatic energy of the lipid layer; it expresses the familiar volume density of the electrostatic energy $\epsilon_W\epsilon_0(\Phi'(x))^2/2$ (where ε_W is the dielectric constant of water, ε_0 is the permittivity of free space, $\Phi(x)$ is the electrostatic potential, and the prime denotes the first derivative) in terms of both the Bjerrum length $l_B = e^2/(4\pi k_B T \epsilon_W \epsilon_0)$ and the dimensionless electrostatic potential $\Psi = e\Phi/k_BT$. To obtain the electrostatic contribution to the average free energy per lipid, we integrate over the x-direction, starting at the polar–apolar interface ($x=0$) and multiply by the (constant) cross-sectional area per lipid, a. The second, third, and fourth terms in Eq. (5) account for the ideal mixing free energy contributions due to the positive salt ions, negative salt ions, and protons, respectively. These three terms alone would adopt a minimum if no compositional gradients were present anywhere in the electrolyte (i.e., for $n_+ = n_0$, $n_- = n_0 + n_p^0$, and $n_p = n_p^0$). The fifth term in Eq. (5) accounts for the energetics of adjusting the protonation/deprotonation equilibrium of PA (corresponding to the reaction $PA^- \rightleftharpoons PA^{2-} + p^+$); here

$$\eta_0 = \frac{1}{1 + 10^{pK-pH}} \tag{6}$$

denotes the intrinsic probability to find PA with two negative charges (PA^{2-}). That is, if the local pH (i.e. the negative decadic logarithm of the *local* proton concentration) is equal to the intrinsic pK, then the degree of deprotonation (i.e. the probability of PA to carry two negative charges) is $\eta_0 = 1/2$. The actual probability η generally differs from the intrinsic probability η_0 due to the influence of the membrane environment on the local proton concentration. We may view any specific choice of η_0 simply as a measure for the pH of the solution through $pH = pK - \ln[(1-\eta_0)/\eta_0)]/\ln 10$. Because the exact value of the intrinsic pK, corresponding to the reaction $PA^- \rightleftharpoons PA^{2-} + p^+$, is not well known, it is convenient to study our model properties directly as function of η_0 with $0 \le \eta_0 \le 1$. The sixth term in Eq. (5) denotes the orientational entropy contribution from the headgroups of the zwitterionic lipids. The integration runs across the headgroup region, $0 \le x \le l$, where in each sub-region $x \ldots x + dx$ there is a constant number of available headgroup orientations $2\pi l dx$. The total number of headgroup orientations, $\int_0^l 2\pi l dx = 2\pi l^2$, thus corresponds to the surface area of a hemisphere. Note that the first six terms in Eq. (5) have been employed in previous work [21], together with an additive non-electrostatic demixing contribution $\sim\phi(1-\phi)$ to the free energy. In the present study we use a more specific non-electrostatic interaction term, one that is not additive but couples with the electrostatic interactions. This contribution is described by the seventh term in Eq. (5). Here, PA^{2-} interacts with the headgroup of the zwitterionic lipid in an orientation-dependent fashion described by the square-well potential $U(x)$ according to Eq. (4). As discussed above, we use this choice to phenomenologically model the formation of a hydrogen bond between the headgroups of PE and PA.

At this point we have fully defined our model. To proceed we note that a number of quantities are free to adjust, namely the local salt concentrations, $n_+(x)$ and $n_-(x)$, the local proton concentration $n_p(x)$, the distribution of headgroup orientations $P(x)$, and the degree of deprotonation η. The free energy $f = f(n_+(x), n_-(x), n_p(x), P(x), \eta)$ must thus adopt its minimum with respect to these unconstrained quantities. The (functional) minimization procedure leads to a number of Boltzmann distributions

$$\begin{aligned} n_+(x) &= n_0\, e^{-\Psi(x)}, \quad n_-(x) = \left(n_0 + n_p^0\right) e^{\Psi(x)}, \\ n_p(x) &= n_p^0\, e^{-\Psi(x)}, \quad P(x) = \frac{1}{q}\, e^{-\Psi(x) + \phi\,\eta\,U(x)}, \end{aligned} \tag{7}$$

where the partition sum

$$q = \frac{1}{l} \int_0^l dx\, e^{-\Psi(x) + \phi\,\eta\,U(x)} \tag{8}$$

ensures the normalization of $P(x)$ according to Eq. (1). In addition, the minimization of f results in the degree of deprotonation of PA

$$\eta = \frac{1}{1 + \frac{1-\eta_0}{\eta_0}\, e^{-\Psi(0) - (1-\phi)\frac{1}{l}\int_0^l dx U(x) P(x)}}. \tag{9}$$

The actual degree of deprotonation (η) is thus equal to the intrinsic degree of deprotonation (η_0) if the electrostatic potential at the headgroup of PA vanishes ($\Psi(x=0)=0$) and if no interaction between PA and PE is present ($U(x)=0$). Below, in Eq. (12), we specify how the intrinsic (η_0) and actual (η) degrees of dissociation relate to the intrinsic and apparent pK.

The distributions $n_+(x)$, $n_-(x)$, $n_p(x)$, $P(x)$, and η still depend on the yet unknown electrostatic potential $\Psi(x)$. We obtain $\Psi(x)$ from the familiar Poisson equation $\Psi''(x) = -4\pi l_B \rho(x)/e$, where we insert into the volume charge density $\rho(x)$, see Eq. (2), the Boltzmann distributions in Eq. (7). This gives rise to the modified Poisson–Boltzmann equation,

$$l_D^2 \Psi'' = \begin{cases} \sinh\Psi - \dfrac{4\pi l_B l_D^2 (1-\phi)}{laq} e^{-\Psi\, +\, \phi\eta U} & 0 < x < l \\ \sinh\Psi & l \le x < \infty. \end{cases} \tag{10}$$

Here, we have introduced the familiar definition $1/l_D^2 = 8\pi l_B (n_0 + n_p^0)$ of the Debye screening length l_D. Salt ions and protons can be present both within and outside the headgroup region. Hence, both lines in Eq. (10) account for their presence (through the term $\sinh\Psi$). The second term in the first line of Eq. (10) accounts for the additional presence of the zwitterionic lipids, which interact with PA^{2-} (present with mole fraction $\eta\phi$) through the non-electrostatic potential $U(x)$. For $\phi = 1$ no zwitterionic lipids are present, and our model reduces to the classical Gouy–Chapman model with a dissociation equilibrium [11]. We note that Eq. (10) needs to be solved with respect to the boundary conditions $\Psi'(x\to\infty) = 0$ and $\Psi'(x=0) = -4\pi l_B \sigma/e$ where the surface charge density σ (measured at $x=0$) is given in Eq. (3). The boundary condition at $x=0$ accounts for the large mismatch in dielectric constants $\epsilon_L \ll \epsilon_W$ within the membrane ($\epsilon_L \approx 4$) and in the aqueous phase ($\epsilon_W \approx 80$). At $x = l$ the potential $\Psi(x)$ needs to be continuous and smooth.

The modified Poisson–Boltzmann equation can be viewed as a self-consistency relation as it usually appears in mean-field models. In our case, Eq. (10) also contains η and thus needs to be solved together with Eq. (9) which, upon inserting the equilibrium expression for $P(x)$ from Eq. (7), becomes a $\Psi(x)$-dependent transcendental equation for η. Solving this system of equations, which is the crucial step for analyzing the implications of the present model, can be accomplished by re-expressing Eqs. (9) and (10) in the form of a Newton–Raphson iteration scheme [12], leading to a sequence of linearized equations that can be solved using standard numerical methods.

The degree of deprotonation η can be expressed by an apparent pK, which we denote by pK_a. The two quantities are related through

$$\eta = \frac{1}{1 + 10^{pK_a - pH}}. \tag{11}$$

We define $\Delta pK = pK_a - pK$, which is the change in the apparent pK value upon exposing PA to both the electrostatic potential of the host membrane and the non-electrostatic interactions with PE. Using Eqs. (6), (9), and (11) we find

$$\begin{aligned} \Delta pK &= \frac{1}{ln10}\, ln\left(\frac{\eta_0(1-\eta)}{\eta\,(1-\eta_0)}\right) \\ &= -\frac{1}{ln10}\left[\Psi(0) + (1-\phi)\frac{1}{l}\int_0^l dx\, U(x) P(x)\right]. \end{aligned} \tag{12}$$

The most simple example is the presence of only PA, corresponding to $\phi = 1$. The second term in the second line of Eq. (12) then vanishes. The negative charges of PA cause a negative potential $\Psi(0)$ and thus a positive shift ΔpK. This is consistent with the interpretation that the negative membrane potential causes additional protonation of PA at fixed pH (as compared to the hypothetical case of vanishing membrane potential). If the zwitterionic lipid is present (i.e., for $\phi<1$), the second term in Eq. (12) will provide a positive contribution (recall that a positive sign of $U(x)$ corresponds to an attractive interaction between PA and the mobile end of the zwitterionic headgroup) and thus tends to *oppose* the positive shift of ΔpK.

3. Results and discussion

Throughout this work we use fixed values for the Bjerrum length $l_B = 0.7$ nm (which expresses the dielectric constant of water $\epsilon w \approx 80$), the cross-sectional area per lipid $a = 0.65\ \mathrm{nm}^2$, the separation of the two opposite charges of the zwitterionic headgroup $l = 0.5$ nm, and the Debye length $l_D = 1$ nm (corresponding to a physiological 0.1 M salt solution). We note that the definition of the Debye length $l_D = [8\pi l_B(n_0 + n_p^0)]^{-1/2}$ also contains the proton concentration, and thus may depend on the pH. However, we safely treat l_D as a constant as long as the bulk salt concentration is much larger than the bulk proton concentration n_p^0. This is certainly fulfilled for all physiologically relevant pH values.

The non-electrostatic attractive potential $-U(x)$ between the phosphomonoester of PA and the hydrogen bond donor at the mobile end of the zwitterionic headgroup is modeled according to the square-well potential in Eq. (4). Our choice of $\tilde{l} = 0.2$ nm reflects a typical effective interaction range of hydrogen bond formation [24]. For the interaction strength we chose $U_0 = 8$ (recall from Eq. (5) that $U(x)$ is expressed in terms of k_BT). This corresponds to ≈ 20 kJ/mol, which is a typical energy scale for hydrogen bond formation [24]. We note that a precise determination of U_0 which accurately accounts for the differences in energy and entropy contained in the hydrogen bond network for x being large ($\tilde{l}<x<l$) and small ($0<x<\tilde{l}$), is beyond the scope of the present work. Yet, different choices of U_0 and $\tilde{l}$ would not qualitatively change our results. (Below, in Fig. 7, we support this assertion by presenting our model predictions for varying choices of U_0 and $\tilde{l}$.) To understand the influence of the ability (PE) or inability (PC) of the zwitterionic headgroup to form a hydrogen bond, we shall compare the two cases $U_0 = 8$ and $U_0 = 0$.

In the following we study the behavior of the mixed lipid layer as a function of the mole fraction ϕ of PA and the intrinsic probability η_0 (which we recall to be a measure of the pH in the solution). We note that η_0 and also ϕ are usually experimentally fixed parameters. Allowing for variations of ϕ (i.e., taking ϕ as a degree of freedom instead of being fixed) would be important in accounting for a tendency of the mixed lipid layer to laterally phase separate. Non-ideal mixing (including phase separation in the presence of calcium ions [25,26] or charged proteins [27]) is, in fact, a relevant subject for membranes that contain PA [28]. As pointed out above, capturing lateral phase separation within the Poisson–Boltzmann framework requires the addition of an appropriate non-ideal mixing term in the free energy that favors phase separation [21]. The present model lacks any such incentive and thus will not predict phase separation.

Fig. 3 shows the degree of deprotonation η as a function of η_0.The left and right diagrams correspond to $U_0 = 0$ and $U_0 = 8$ respectively; the curves in each diagram represent different mole fractions ϕ of PA (with $\phi = 0$, $\phi = 0.1$, $\phi = 0.2$, $\phi = 0.3$, $\phi = 0.4$, $\phi = 0.5$, $\phi = 0.7$, $\phi = 1$ from top to bottom).

For $\phi = 1$ the lipid layer contains only PA. In the absence of zwitterionic headgroups that potentially act as hydrogen bond donors, the potential $U(x)$ becomes irrelevant and the curves in both diagrams must be identical. According to Eq. (9) the two limiting values $\eta_0 = 0$ and $\eta_0 = 1$ always fix the corresponding degree of deprotonation, $\eta = 0$ and $\eta = 1$, respectively. Yet, in between, η tends to remain close to zero. The interpretation is straightforward: the negative potential $\Psi(x = 0)$ at the headgroup of PA attracts protons, and this shifts the equilibrium of the protonation/deprotonation reaction $PA^- \rightleftharpoons PA^{2-} + p^+$ towards the protonated state PA^-.

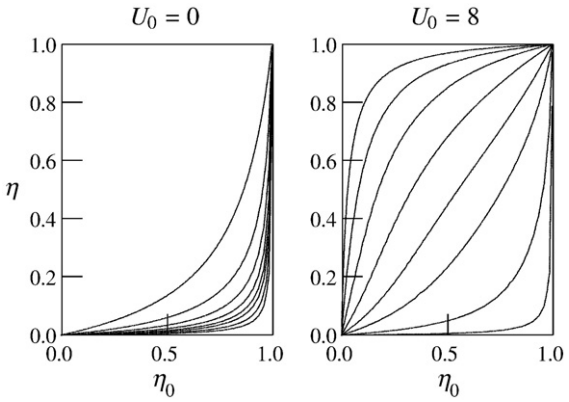

Fig. 3. The degree of deprotonation η as a function of η_0 (which is related to the pH and pK of PA according to Eq. (6)) for various mole fractions of PA: $\phi = 0$, $\phi = 0.1$, $\phi = 0.2$, $\phi = 0.3$, $\phi = 0.4$, $\phi = 0.5$, $\phi = 0.7$, $\phi = 1$ from top to bottom. As indicated, the left diagram corresponds to $U_0 = 0$, and the right diagram to $U_0 = 8$.

For $\phi<1$ the choices $U_0 = 0$ and $U_0 = 8$ lead to significantly different results. Consider first the case $U_0 = 0$ (left diagram): Here, the addition of zwitterionic lipids (decreasing ϕ) increases η only moderately. Replacing PA by a zwitterionic lipid exchanges the possibly two negative charges of PA by one single negative charge, namely the phosphate group of the zwitterionic lipid. The potential $\Psi(0)$ remains negative, although less negative than for $\phi = 1$. The negative potential $\Psi(0)$ implies $\eta<\eta_0$; see Eq. (9) for $U(x) = 0$. This consideration also applies to the case $\phi \to 0$ where PA is present in the dilute limit (thus acting as a probe molecule). To sum up, for $U_0 = 0$ we always find $\eta<\eta_0$ which simply reflects the negative sign of the membrane potential. Consider now the other case, $U_0 = 8$ (right diagram): Here, the zwitterionic headgroup acts as a hydrogen bond donor. Hydrogen bond formation leaves PA in its deprotonated state, thus increasing η. In addition, hydrogen bond formation requires close proximity of the positively charged end of the zwitterionic headgroup to the headgroup of PA. This proximity of positive charge renders the potential $\Psi(0)$ more positive, further facilitating the state PA^{2-} over PA^-. In the excess of zwitterionic lipids (small ϕ), almost all PA will be subject to hydrogen bond formation, implying large η. In this case it is $\eta>\eta_0$ despite the negative potential $\Psi(0)$. For $\phi = 0.4$ we find approximatively $\eta = \eta_0$; here the negative potential $\Psi(0)$ and the tendency to form hydrogen bonds compensate each other, implying $\Psi(0) \approx -(1-\phi)(1/l)\int_0^l dx\, U(x)P(x)$ for any choice of ϕ.

The dependence $\eta = \eta(\eta_0, \phi)$, plotted in Fig. 3, can be used to calculate the shift ΔpK according to Eq. (12). This is displayed in Fig. 4. Again, the results for $U_0 = 0$ and $U_0 = 8$ must converge at $\phi = 1$ where no zwitterionic lipids (and thus no hydrogen bond formations) are present. In addition, ΔpK always (for both $U_0 = 0$ and $U_0 = 8$) increases with ϕ; this is implied by the decrease of η with growing ϕ (see Fig. 3). For $U_0 = 0$ (broken lines in Fig. 4) the shift ΔpK is always positive. This reflects the negative potential $\Psi(0)$ which favors the protonated state PA^- over PA^{2-}. For $U_0 = 8$ (solid lines in Fig. 4) the shift ΔpK is negative for $\phi \lesssim 0.4$ and positive for $0.4 \lesssim \phi$. Recall from the discussion of Fig. 3 that at about $\phi = 0.4$ the negative potential $\Psi(0)$ and the tendency to form hydrogen bonds compensate each other, leading to $\eta \approx \eta_0$ and hence $\Delta pK \approx 0$. We also note that the total changes of ΔpK are large for $U_0 = 8$, spanning about four pH units within the range $0 \le \phi \le 1$. The ionization state of PA thus depends sensitively on the mole fraction of potential hydrogen bond donors (in

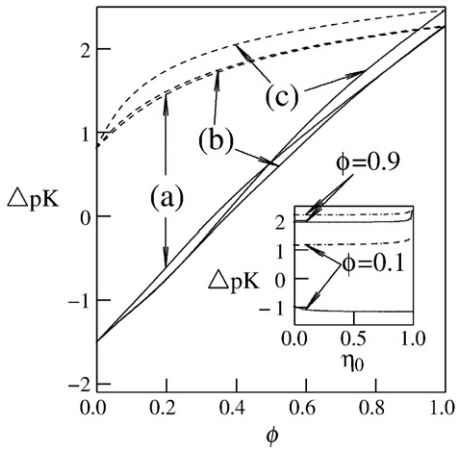

Fig. 4. ΔpK (see Eq. (12)) as function of ϕ for $\eta_0=0.1$ (a), $\eta_0=0.7$ (b), and $\eta_0=0.99$ (c). The inset shows ΔpK vs. η_0 for fixed ϕ as indicated. In all cases broken lines correspond to $U_0=0$ and solid lines to $U_0=8$.

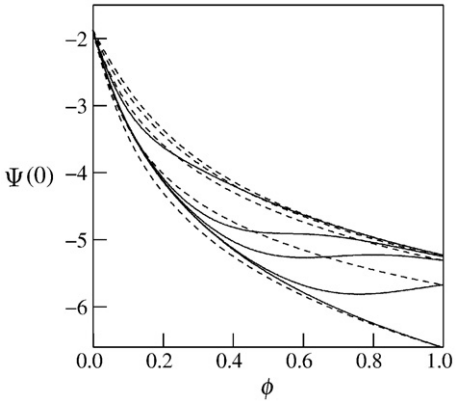

Fig. 5. Dimensionless electrostatic potential $\Psi(x=0)$ at the polar/apolar interface (at $x=0$) as a function of ϕ for $\eta_0=0.1$, $\eta_0=0.7$, $\eta_0=0.9$, $\eta_0=0.99$, and $\eta_0=1$; from top to bottom. The broken lines correspond to $U_0=0$, and the solid lines to $U_0=8$.

our model the zwitterionic headgroups). The large shifts of ΔpK with composition ϕ are a consequence of the electrostatic–hydrogen bond switch mechanism; these shifts are much larger than those that could realistically be achieved by a regulation entirely through the electrostatic potential. The large changes in ΔpK as function of the availability of hydrogen bond donors is likely to be a key for the ability of proteins to specifically interact with (and thus sequester) PA.

It is interesting to note that ΔpK can be calculated analytically in two limiting cases. Namely, for $\eta_0=0$ and $\phi=1$ the membrane contains only PA^-, whereas for $\eta_0=1$ and $\phi=1$ it only consists of PA^{2-}. As is well known [29], the (dimensionless) potential $\Psi(0)$ at a planar surface with surface charge density $\sigma=-ze/a$ (where z denotes the valence of the charge) is -2 arsinh $(2z\pi l_B l_D/a)$ (this is one of the few analytical results of the classical non-linear Poisson Boltzmann model). Hence for PA^- we obtain $\Psi(0)=-2$ arsinh $(2\pi l_B l_D/a)=-5.2$, implying $\Delta pK=-\Psi(0)/\ln 10=2.26$. Similarly, for PA^{2-} we find $\Psi(0)=-2$ arsinh $(4\pi l_B l_D/a)=-6.6$ and thus $\Delta pK=2.87$. We see that increasing η_0 from $\eta_0=0$ to $\eta_0=1$ (at fixed $\phi=1$) increases ΔpK from 2.26 to 2.87. In other words, a very large increase in pH (which changing η_0 from 0 to 1 corresponds to) leads to a small increase in ΔpK. This is notable because both the pK and pK_a represent equilibrium constants, implying that the pH—while affecting the protonation/deprotonation state—should not influence ΔpK. Yet, in our present model the pK_a does depend on the pH value which is a result of the pH-induced modifications of the electrostatic and structural properties of the membrane. However, the pH-dependent changes of ΔpK are small, and they remain so for all η_0 irrespective of U_0. The weak dependence of ΔpK as function of η_0 is demonstrated in the inset of Fig. 4, thus supporting the usefulness of introducing an apparent pK that is independent of the ambient pH.

Another quantity that our model predicts is the (dimensionless) electrostatic potential $\Psi(0)$, measured at the polar/apolar interface $x=0$. Fig. 5 shows $\Psi(0)$ as function of ϕ. For $U_0=0$ (broken lines) the potential decreases monotonously with growing ϕ and η. As mentioned above, growing ϕ corresponds to replacing the one single negative charge of the zwitterionic lipid at $x=0$ by potentially two negative charges of PA. More negative charge then lowers the potential $\Psi(0)$. The situation is different for $U_0=8$. Here, the mixture of PA with zwitterionic lipids leads to hydrogen bond formation, thus favoring the deprotonated state with a corresponding lower potential. This may even lead to a local minimum in $\Psi(0)$ at intermediate values of ϕ where hydrogen bonding is most efficient (see Fig. 5). We recall from above that for $\phi=1$ the potentials $\Psi(0)=-5.2$ for $\eta_0=0$ and $\Psi(0)=-6.6$ for $\eta_0=1$ can be expressed analytically, because these cases correspond to a single charged surface with fixed surface charge densities $\sigma=-e/a$ (for PA^-) and $\sigma=-2e/a$ (for PA^{2-}), respectively.

The final quantity that our model predicts is the probability distribution $P(x)$ of zwitterionic headgroup orientations. An example, derived for $\eta_0=0.7$ and $\phi=0.5$, is shown in Fig. 6. For $U_0=0$ (broken line) the probability $P(x)$ is largest close to $x=0$ due to the electrostatic attraction between the negative charge(s) of the phosphomonoester and the positive charge of the mobile end of the zwitterionic headgroup. Without this electrostatic attraction the headgroup's orientational entropy would cause a uniform distribution $P(x)=1$. For $U_0=8$ (solid line) the additional tendency to form a hydrogen bond favors large headgroup angles $\theta\approx\pi/2$ (see Fig. 2) even more. The probability $P(x)$ in Fig. 6 exhibits an almost step-like decay at $x=\tilde{l}=0.2$ nm, where we recall that $\tilde{l}$ sets the range of attraction for the formation of a hydrogen bond in our present model. Orientations with $x>\tilde{l}$ have an essentially vanishing probability.

The probability $P(x)$ can be used to calculate the average position

$$\langle x\rangle = \frac{1}{l}\int_0^l \mathrm{d}x\, P(x)x \tag{13}$$

of the mobile end of the zwitterionic headgroup along the x-axis. The results are shown in the inset of Fig. 6. Without any interactions we would find constant $P(x)\equiv 1$ and thus $\langle x\rangle=0.25$. The actual value of $\langle x\rangle$ is smaller than 0.25 because of the electrostatic attraction between

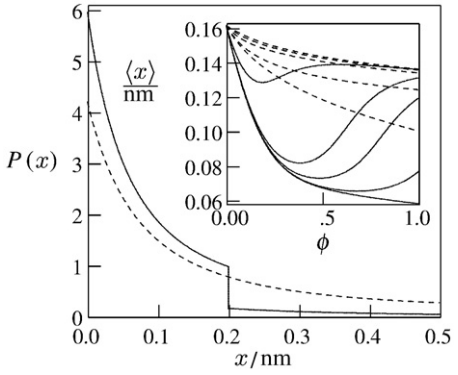

Fig. 6. The probability $P(x)$ for $\eta_0=0.7$ and $\phi=0.5$. *Inset*: Average position $\langle x\rangle$ of the mobile (positively charged) end of the zwitterionic headgroup as a function of ϕ for $\eta_0=0.1$, $\eta_0=0.7$, $\eta_0=0.9$, $\eta_0=0.99$, and $\eta_0=1$, from top to bottom. In both the main diagram and the inset broken lines correspond to $U_0=0$ and solid lines to $U_0=8$.

the positive charge of the zwitterionic headgroup and the negative charges at $x=0$. For $U_0=0$ the value of $\langle x\rangle$ decreases monotonously as function of growing ϕ and η. In this case, the tilting of the headgroup (larger θ) can be understood completely in terms of an increased electrostatic interaction. For $U_0=8$ the tendency to form a hydrogen bond leads to a substantially more pronounced headgroup tilt angle (i.e., smaller $\langle x\rangle$). For intermediate η_0 the average $\langle x\rangle$ (ϕ) passes through a minimum; this reflects the competitive tendencies of the phosphomonoester to undergo hydrogen bond formation or to get protonated. The latter, which releases the headgroup, dominates at large ϕ because the number of zwitterionic headgroups (hydrogen bond donors) becomes small.

We finally discuss how the predictions of our model are influenced by the choice of the parameters U_0 and $\tilde{l}$ in the square-well potential $-U(x)$ (see Eq. (4)). Recall that the depth U_0 and width $\tilde{l}$ of the square-well represent phenomenological parameters whose magnitudes are not obvious to estimate within the Poisson–Boltzmann framework (see also the discussion in Appendix A). In Fig. 7 we display the influence of U_0 and $\tilde{l}$ on ΔpK (for fixed $\eta_0=0.7$ in all cases). The three sets of solid curves correspond to $U_0=3$ (a), $U_0=8$ (b), and $U_0=16$ (c). Each set contains three solid curves, derived for $\tilde{l}=0.1$, $\tilde{l}=0.2$, $\tilde{l}=0.3$. Comparison to the absence of hydrogen bond formation ($U_0=0$; the dashed line in Fig. 7) shows that the qualitative predictions of our model are not affected by the specific choices of U_0 and $\tilde{l}$. That is, the electrostatic–hydrogen bond switch generally increases the sensitivity of the dissociation state of PA with respect to the PA/PE ratio present in the membrane. For larger U_0 the changes in ΔpK as function of ϕ become larger whereas the influence of $\tilde{l}$ is small. We also point out that the cross-sectional area per lipid a has a minor influence on ΔpK. This is exemplified by the dotted line in Fig. 7 which was calculated for $a=0.45\text{nm}^2$ (all other result in this work refer to $a=0.65\text{nm}^2$).

4. Conclusions

In summary, despite the negative potential $\Psi(0)$ at the headgroup of PA, the membrane-induced change in pK value, ΔpK, can be negative as a result of the electrostatic–hydrogen bond switch mechanism. Concomitantly, the changes of ΔpK as function of membrane composition ϕ are large, spanning several pH units. Hence, membrane composition (or, more generally, the availability of hydrogen bond donors for the phosphomonoester head group of PA) serves as an efficient regulator of the charging state of PA. This mechanism may contribute to the specific binding between PA and proteins that possess hydrogen bond donating groups.

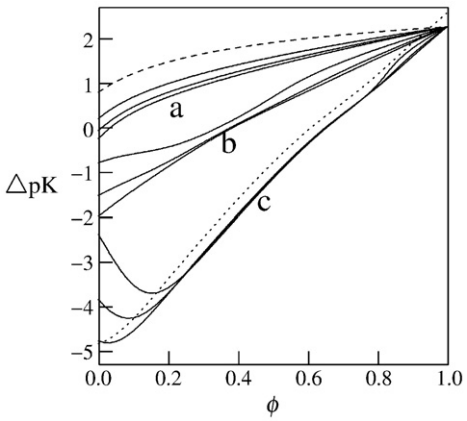

Fig. 7. ΔpK (see Eq. (12)) as function of ϕ for fixed $\eta_0=0.7$. The three sets of solid curves correspond to $U_0=3$ (a), $U_0=8$ (b), and $U_0=16$ (c), each derived for $\tilde{l}=0.1$, $\tilde{l}=0.2$, $\tilde{l}=0.3$ (in the small ϕ region from top to bottom). The dashed line corresponds to $U_0=0$. The dotted line is for $U_0=16$, $\tilde{l}=0.3$, and $a=0.45\text{nm}^2$.

The present work suggests that even complex regulating mechanisms, such as the electrostatic–hydrogen bond switch, can be captured qualitatively using the classical Gouy–Chapman approach, given that appropriate modifications are introduced. The key modifications in the present study are the (phenomenological) account of hydrogen bond formation through the square-well potential $-U(x)$ and the structural model for a zwitterionic lipid headgroup (with its orientational degree of freedom θ). It should be pointed out that our modified Gouy–Chapman approach represents a minimal model that lacks any atomistic detail and thus aims at a qualitative understanding instead of a quantitative description (for which atomistic simulations are much more appropriate). This is even more so because our results are also subject to the familiar approximations of the Gouy–Chapman approach, namely the absence of electrostatic correlations, its continuum level description, the modeling of all involved ions as point charges, and the neglect of the solvent structure. In addition, any variations of the system properties in the lateral membrane direction are ignored. This includes variations of the electrostatic potential in the $x\equiv 0$ plane which arise from the discreteness of the surface charges [30]. Strictly then, these variations may lead to correlations between lipids, mediated for example by the bridging of the cationic end of the zwitterionic lipid headgroup to the anionic charge of a neighboring lipid. These effects would only be insignificant if the headgroup length l was large compared to the distance $\sqrt{a}$ between neighboring lipids. In our model the two distances are comparable which thus will affect the system properties to some extent (for a comparison of the present Poisson–Boltzmann model for zwitterionic lipids with Monte Carlo simulations see [16]). Despite these inherent limitations it is striking that the sensitive regulation of headgroup charge, via the formation of a hydrogen bond, is captured by our model. An understanding of the electrostatic–hydrogen bond switch by calculations such as these should lead to a better appreciation of the sensitive mechanisms influencing PA–protein interactions. In the case of Opi1 it is likely that binding to PA is facilitated by the electrostatic–hydrogen bond mechanism. The corresponding regulation of the protein binding strength via relatively small changes in the intracellular pH effectively links metabolism and membrane biogenesis by utilizing the ionization properties of the simplest glycerol-phospholipid, PA.

Acknowledgment

SM thanks the NSF for support through grant DMR-0605883. EEK was supported by a Farris Family Fellowship and Kent State University.

Appendix A

Some force fields in molecular simulations (such as AMBER) employ a 10–12 potential to describe the energetics of hydrogen bond formation [23]. The 10–12 interaction potential can be expressed as

$$U_{10-12}(x)=\tilde{U}\left[-6\left(\frac{\tilde{x}}{x}\right)^{10}+5\left(\frac{\tilde{x}}{x}\right)^{12}\right] \tag{14}$$

where x is the distance between the hydrogen atom and the hydrogen bond acceptor, $\tilde{U}$ is the depth of the energy minimum (i.e., the strength of the hydrogen bond), and $\tilde{x}$ the corresponding optimal distance. The 10–12 interaction potential in Eq. (14) is plotted in Fig. 8. In our present work we have used a square-well function $-U(x)$ to approximate $U_{10-12}(x)$. Recall that $U(x)$ is characterized by the two parameters U_0 and $\tilde{l}$; see Eq. (4). Let us choose these two parameters so that $-U(x)$ best approximates $U_{10-12}(x)$. To this end we first note that $U_{10-12}(x)=0$ for $x/\tilde{x}=\sqrt{5/6}=0.913$. We place the left border of the square-well at this position (see Fig. 8). Scaled

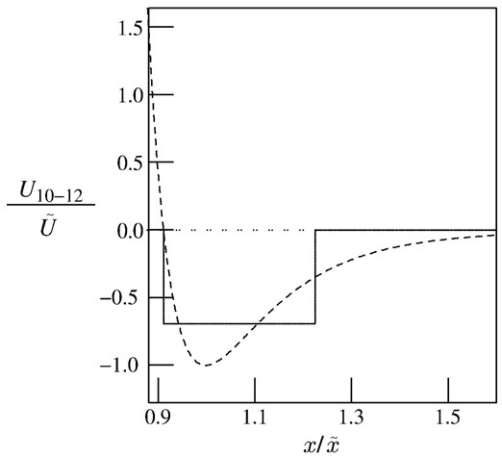

Fig. 8. The scaled 10–12 interaction potential $U_{10-12}/\tilde{U}$ according to Eq. (14) (dashed line) and the corresponding optimal (scaled) square-well potential $-U(x)/\tilde{U}$ (solid line). Width and depth of the optimal square-well are $0.314\tilde{x}$ and $0.692\tilde{U}$, respectively.

depth ($U_0/\tilde{U}$) and width ($\tilde{l}/\tilde{x}$) of the square-well can then be found by numerically minimizing the integral

$$\int_{\sqrt{\frac{5}{6}}\tilde{x}}^{\infty} dx[U_{10-12}(x) + U(x)]^2 \tag{15}$$

The result is

$$U_0 = 0.692\,\tilde{U}, \quad \tilde{l} = 0.314\,\tilde{x} \tag{16}$$

The resulting function $-U(x)/\tilde{U}$ is plotted together with $U_{10-12}(x)/\tilde{U}$ in Fig. 8. Hence, for any choice of the two parameters $\tilde{U}$ and $\tilde{x}$ in Eq. (14) we can formally find the corresponding values for U_0 and $\tilde{l}$ of the square-well potential $-U(x)$. It should be pointed out, however, that the present Poisson–Boltzmann approach neglects the steric size of all involved ions. That is, the attractive part of the square-well potential $-U(x)$ starts at $x=0$ whereas $U_{10-12}(x)$ is repulsive for $0 \le x \le \sqrt{5/6}\,\tilde{x}$ and becomes attractive only for $x > \sqrt{5/6}\,\tilde{x}$. The neglect of the steric ion sizes in the Poisson–Boltzmann model might be compensated for by assigning a larger value to $\tilde{l}$ than given in Eq. (16), but the optimal choice is not obvious.

References

[1] T.G. Kutateladze, Mechanistic similarities in docking of the FYVE and PX domains to phosphatidylinositol 3-phosphate containing membranes, Prog. In Lipid Res. 46 (6) (2007) 315–327.
[2] M.A. Lemmon, Pleckstrin homology (PH) domains and phosphoinositides, Cell Biol. Inositol Lipids Phosphates 74 (2007) 81–93.
[3] T. Yeung, G.E. Gilbert, J. Shi, J. Silvius, A. Kapus, S. Grinstein, Membrane phosphatidylserine regulates surface charge and protein localization, Science 319 (5860) (2008) 210–213.
[4] E.E. Kooijman, D.P. Tieleman, C. Testerink, T. Munnik, D.T.S. Rijkers, K.N.J. Burger, B. de Kruijff, An electrostatic/hydrogen bond switch as the basis for the specific interaction of phosphatidic acid with proteins, J. Biol. Chem. 282 (15) (2007) 11356–11364.
[5] E. Kooijman, C. Testerink, Phosphatidic acid: an electrostatic/hydrogen-bond switch? in: T. Munnik (Ed.), Lipid Signaling in Plants, Vol. 16 of Plant Cell Monographs, Springer Berlin / Heidelberg, 2010, pp. 203–222.
[6] B.P. Young, J.J.H. Shin, R. Orij, J.T. Chao, S.C. Li, X.L. Guan, A. Khong, E. Jan, M.R. Wenk, W.A. Prinz, G.J. Smits, C.J.R. Loewen, Phosphatidic acid is a pH biosensor that links membrane biogenesis to metabolism, Science 329 (5995) (2010) 1085–1088.
[7] S. McLaughlin, The electrostatic properties of membranes, Ann. Rev. Biophys. Biophys. Chem. 18 (1989) 113–136.
[8] D. Andelman, Electrostatic properties of membranes: the Poisson–Boltzmann theory, in: R. Lipowsky, E. Sackmann (Eds.), 2nd Edition, Structure and Dynamics of Membranes, 1, Elsevier, Amsterdam, 1995, pp. 603–642,, section 12.
[9] S. Lifson, A. Katchalsky, The electrostatic free energy of polyelectrolyte solutions: ii. Fully stretched macromolecules, J. Polymer Sci. 13 (1954) 43–55.
[10] H.N.W. Lekkerkerker, Contribution of the electric double layer to the curvature elasticity of charged amphiphilic monolayers, Phys. A. 159 (1989) 319–328.
[11] B.W. Ninham, V.A. Parsegian, Electrostatic potential between surfaces bearing ionizable groups in ionic equilibrium with physiologic saline solution, J. Theor. Biol. 31 (3) (1971) 405–428.
[12] D. Harries, S. May, W.M. Gelbart, A. Ben-Shaul, Structure, stability and thermodynamics of lamellar DNA-lipid complexes, Biophys. J. 75 (1998) 159–173.
[13] I. Borukhov, D. Andelman, H. Orland, Polyelectrolyte solutions between charged surfaces, Europhysics Lett. 32 (6) (1995) 499–504.
[14] E. Ruckenstein, M. Manciu, The coupling between the hydration and double layer interactions, Langmuir 18 (20) (2002) 7584–7593.
[15] A. Abrashkin, D. Andelman, H. Orland, Dipolar Poisson–Boltzmann equation: ions and dipoles close to charge interfaces, Phys. Rev. Lett. 99 (7) (2007) 077801.
[16] E.C. Mbamala, A. Fahr, S. May, Electrostatic model for mixed cationic–zwitterionic lipid bilayers, Langmuir 22 (11) (2006) 5129–5136.
[17] D.H. Mengistu, S. May, Debye–Huckel theory of mixed charged-zwitterionic lipid layers, Eur. Phys. J. E 26 (3) (2008) 251–260.
[18] D.H. Mengistu, S. May, Nonlinear Poisson–Boltzmann model of charged lipid membranes: accounting for the presence of zwitterionic lipids, J. Chem. Phys. 129 (12) (2008) 121105.
[19] A. Haugen, S. May, The influence of zwitterionic lipids on the electrostatic adsorption of macroions onto mixed lipid membranes, J. Chem. Phys. 127 (21) (2007) 215104.
[20] D.H. Mengistu, K. Bohinc, S. May, Binding of DNA to zwitterionic lipid layers mediated by divalent cations, J. Phys. Chem. B 113 (36) (2009) 12277–12282.
[21] D.H. Mengistu, K. Bohinc, S. May, A model for the electrostatic contribution to the pH-dependent nonideal mixing of a binary charged-zwitterionic lipid bilayer, Biophys. Chem. 150 (1–3) (2010) 112–118.
[22] E.E. Kooijman, K.M. Carter, E.G. van Laar, V. Chupin, K.N.J. Burger, B. de Kruijff, What makes the bioactive lipids phosphatidic acid and lysophosphatidic acid so special? Biochem. 44 (51) (2005) 17007–17015.
[23] A.K. Pappe, C.J. Casewit, Molecular Mechanics across Chemistry, University Science Books, 1996.
[24] P.R. Bergethon, The Physical Basis of Biochemistry: The Foundations of Molecular Biophysics, Springer Verlag, 1998.
[25] K.K. Eklund, J. Vuorinen, J. Mikkola, J.A. Virtanen, P.K.J. Kinnunen, Ca-2+-induced lateral phase-separation in phosphatidic-acid phosphatidylcholine monolayers as revealed by fluorescence microscopy, Biochem. 27 (9) (1988) 3433–3437.
[26] J. Faraudo, A. Travesset, Phosphatidic acid domains in membranes: effect of divalent counterions, Biophys. J. 92 (8) (2007) 2806–2818.
[27] M.D. Bazzi, G.L. Nelsestuen, Extensive segregation of acidic phospholipids in membranes induced by protein-kinase-c and related proteins, Biochem. 30 (32) (1991) 7961–7969.
[28] P. Garidel, C. Johann, A. Blume, Nonideal mixing and phase separation in phosphatidylcholine phosphatidic acid mixtures as a function of acyl chain length and pH, Biophys. J. 72 (5) (1997) 2196–2210.
[29] D.F. Evans, H. Wennerström, The Colloidal Domain, Where Physics, Chemistry, and Biology Meet, 2nd Edition, VCH publishers, 1994.
[30] A.P. Nelson, D.A. McQuarrie, Effect of discrete charges on electrical properties of a membrane .1, J. Theoretical Biol. 55 (1) (1975) 13–27.